Fundamentals and applications of silica and non-silica holey fibers

Heike Ebendorff-Heidepriem*, Kentaro Furusawa, David R. Richardson, Tanya M. Monro

Optoelectronics Research Centre, University of Southampton, SO17 1BJ, United Kingdom

ABSTRACT

Microstructured optical fibers are of increasing interest since they offer unique optical properties and design flexibility that cannot be achieved in conventional forms of fiber. We review structural features, fabrication, optical properties and potential applications of index-guiding holey optical fibers. The state-of-the-art is presented for both silica and compound glass holey fibers.

Keywords: microstructured optical fibers, holey optical fibers, photonic crystal optical fibers, fiber design and fabrication, nonlinear fiber devices

1. INTRODUCTION

The microstructured fiber (MF) is a new class of optical fiber that has emerged in recent years [1-6]. They have attracted increasing attention because they offer unique optical properties and design flexibility that cannot be provided by conventional optical fibers, and this opens up diverse potential applications in telecommunications, metrology, medicine and beyond. Microstructured fibers contain an arrangement of holes running along the fiber length. The vast majority of microstructured fibers produced to date are air/silica MFs that contain air holes embedded in undoped silica glass [1-6]. Recently, compound glasses with high optical nonlinearity (lead-silicate, tellurite, bismuth-oxide) have gained attraction for MFs [7-13]. In addition, polymer-based MFs have been reported [14]. In contrast to conventional fibers, MFs can be made from a single material which eliminates the problems induced by the core/cladding interface of two different glasses. However, MFs are not limited to air/solid structures. Very recently, a glass/glass MF or so called all-solid holey fiber has been demonstrated [15]. In this MF type, lower index glass inclusions representing the holes are embedded in a higher-index matrix. The design flexibility of MFs is based on the freedom in the specification of the size, shape and arrangement of the holes combined with the flexibility in the properties of the solid material. A range of MF geometries is illustrated in figure 1.

The holes within the MFs act as fiber cladding, and light can be guided using either one of two quite different mechanisms. Index-guiding MFs guide light due to the principle of modified total internal reflection, and such fibers are widely known as holey fibers (HFs) [2]. The holes act to lower the effective refractive index in the cladding region, and so light is confined within the solid core, which has a relatively higher index. The basic operation of index-guiding fibers does not depend on having a periodic array of holes [16]. However, in practice the holes are typically arranged on a hexagonal lattice, and so these fibers are also often referred to as photonic crystal fibers [3,4]. The effective refractive index of the cladding can vary strongly as a function of the wavelength of light guided by the fiber. In addition, the optical properties of index-guiding HFs are determined by the configuration of air holes used to form the cladding, and many different arrangements can be envisaged within this flexible fiber type. For these reasons, it is possible to design fibers with spectrally unique properties not possible in conventional fibers such as broadband single-mode guidance, anomalous dispersion at wavelengths down to 560nm, large normal dispersion at 1550nm and high form birefringence. Simply by scaling the dimensions of the features within the fiber profile, HFs can have mode areas ranging three orders of magnitude. HFs with large mode area are of great interest for high power transmission systems and high power lasers [17-25]. At the other extreme, HFs with small mode area have a large nonlinearity which has been used in a variety of nonlinear devices for wavelength conversion, supercontinuum generation, all-optical switching, pulse compression, soliton formation and beyond [26-62].

* heh@orc.soton.ac.uk; phone 44-2380-592825; fax 44-2380-593149

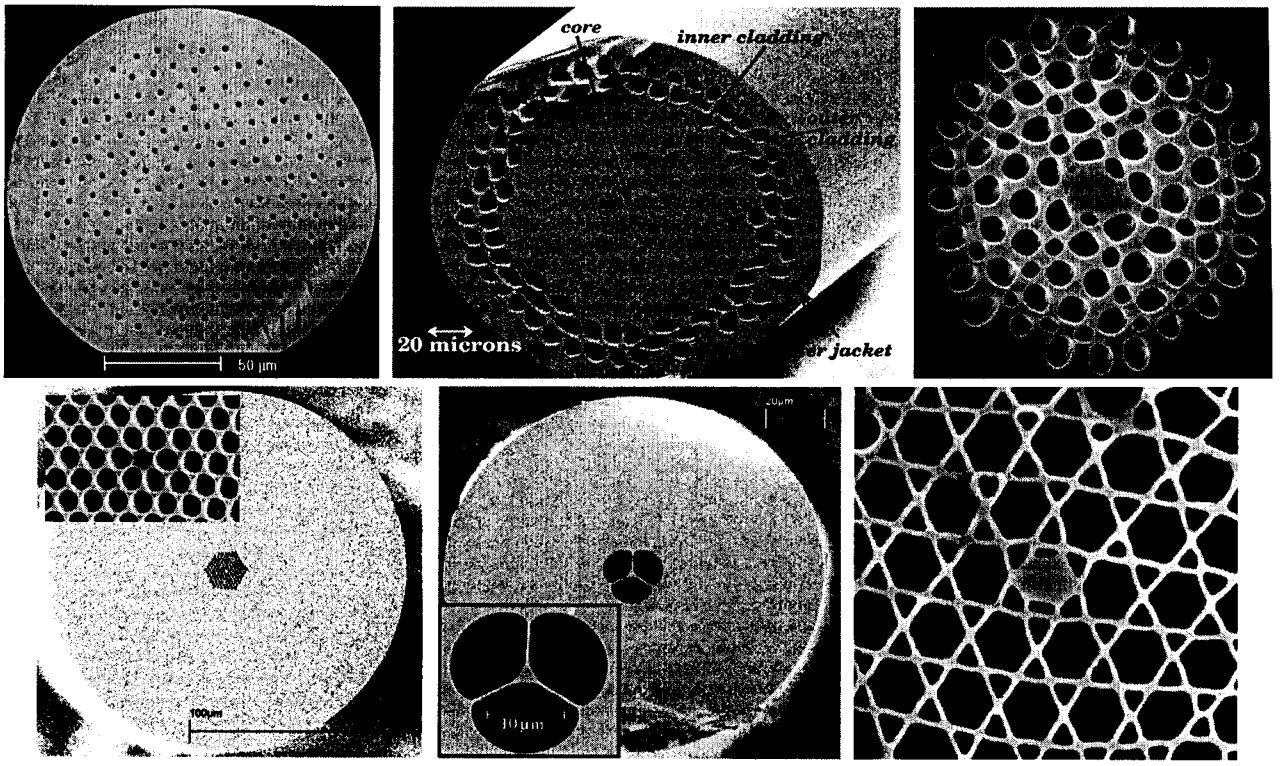

Fig. 1. SEM images of various HFs: (a) large mode area silica HF with 15µm core, (b) large mode area double-clad Yb-doped silica HF with 17µm core, (c) small core highly nonlinear silica HF with ~1.5µm core and asymmetric hole arrangement, (d) small core highly nonlinear silica HF with 1.2µm core, (e) small core highly nonlinear lead-silicate HF with 1.7µm core, (f) small core Yb-doped silica HF with elliptical core of 1.5×2.6µm.

MFs can guide light by an alternative guidance mechanism, the so called photonic bandgap effect, if the air holes that define the cladding are arranged on a periodic lattice [3-6]. Periodic cladding structures can exhibit photonic bandgaps, and frequencies located in the bandgap are trapped in the core and cannot propagate within the cladding. By suitably breaking the periodicity of the cladding (e.g. by adding extra holes to form a low-index defect), it is possible to introduce a localized mode within this defect. Such a defect can act as a core, and guide light within well-defined frequency windows. Photonic bandgap fibers with air hollow cores can be designed to have transmission windows centered at near-infrared wavelengths and are of particular interest for gas/light interactions and the transport of high intensity optical fields [4]. The prospects of photonic bandgap fibers with a lower transmission loss than conventional fibers represent a tantalizing possibility with the potential to revolutionize telecommunications.

In addition to single-material holey and photonic bandgap fibers, in which the light is solely confined by the holes in the cladding, hybrid MFs exist, which combine a high-index (doped) core with a holey cladding. At one extreme, in air-clad or hole-assisted fibers, the light is guided in the higher index core surrounded by the lower index solid cladding like in conventional fibers [63-67]. In hole-assisted fibers, the air holes in the cladding subtly modify the guidance properties such as dispersion [63], or they affect the cladding modes in fiber gratings [64]. Filling the holes with active materials such as polymers opens up the development of tunable grating filters [64,65]. In air-clad fibers, the outer cladding with a high air-filling fraction creates a high numerical aperture inner cladding which is of importance for cladding-pumped high power lasers [66,67]. Alternatively, dopants are used in the core of a HF to create active HFs. In such cases, it is often desirable to ensure that the guidance is dominated by the holes and the dopant is just there to create an active medium [23-25].

In this paper, we review fabrication, fundamental properties and device applications of index-guiding HFs made from silica or compound glass. In section 2, we describe the techniques and challenges for HF fabrication. In section 3, basic waveguiding properties and their dependence on HF geometry are reviewed. Section 4 gives an overview on practical applications of HFs and describes selected device applications.

2. FABRICATION

The vast majority of HF preforms produced to date have been fabricated using stacking techniques. Capillary tubes are stacked in a hexagonal configuration, and the central capillary can then be replaced with a solid glass rod, which ultimately forms the fiber core. The stacking procedure is a flexible one: HFs suitable for active devices can be made using rare-earth-doped core rods [23-25,68-72]. Special core shapes can be produced by introducing multiple rods in the stack [21,24,73,74]. Off-center cores can be readily made by replacing a non-central capillary [23,25]. Multiple interacting or non-interacting cores can be made by replacing multiple capillaries which have a larger or smaller distance between them [75,76]. Elliptical cores can be formed by using capillaries with different hole sizes [27,49,69,70,77-79]. In addition, very regular structures can be made [80], or asymmetric hole arrangements can be achieved [27]. In active HFs with high doping levels, two different approaches have been used to minimize the step-index between doped core region and cladding and thus to ensure that the guidance is dominated by the holes. Either a lower-index codopant [24] or a composite core rod that contains an ensemble of small doped regions [25] have been employed. The reproducibility of the structured profile in the preform depends on having long uniform capillaries to stack and achieving a good stacking configuration with many tubes. The drawback of stacking is that the preform fabrication is labor-intensive.

Recently, the use of compound glass with low softening temperatures has allowed to develop the extrusion technique for fabrication of structured preforms [7-13]. In this process, a glass billet is forced through a die at elevated temperatures near the softening point, whereby the die orifice determines the preform geometry. Once the optimum die geometry and process parameters have been established, the preform fabrication process can be automated. In this way good reproducibility in the preform geometry has been achieved [12]. The advantage of the extrusion technique is that the preform for the microstructured part of a fiber can be produced in one step without stacking.

For larger scale features, fibers are drawn directly in a single step from the preform. For small scale features, the preform is first reduced to a cane of 1-2mm diameter on a drawing tower, and in a second step this cane is inserted in a solid jacketing tube and then drawn to the final fiber. One of the most challenging aspects of air/glass HF fabrication is to prevent collapse of the holes and to achieve the desired hole size and shape during caning and fiber drawing. The microstructured profile is affected by the pressure inside the holes, surface tension of the glass and temperature gradient in the preform. The drawing process of air/silica HFs has now developed to a degree where the cladding configuration can be controlled relatively well by careful choice of the process parameters. As a result, km scale lengths of fibers with small variations in the HF geometry (~1%) have been achieved. In addition, protective polymer coatings are applied, which makes HFs more robust and their use more practical. From a practical perspective it is important to note that silica HFs can be directly spliced to conventional fiber types using conventional cleaving/splicing approaches [81-83].

To date extrusion and fiber drawing of compound glass HFs is still at an early stage of development. In addition, the much steeper viscosity curves of soft glasses compared with silica glass make greater demands on the process control. Nevertheless, a high degree in the reproducibility of the HF geometry has already been demonstrated for a lead silicate glass [12].

3. BASIC PROPERTIES AND MODELLING

The parameters that characterize a HF profile with circular air holes arranged on a hexagonal lattice and that determine their optical properties are the hole-to-hole spacing Λ, the hole diameter d, the relative hole size d/Λ or air-filling fraction and the number of rings of holes used to define the cladding. The effective index difference between core and cladding is a strong function of wavelength, since at longer wavelengths the field extends further into the air holes thereby reducing the effective cladding index. This results in a range if unique and potentially useful properties, which can be tailored via the HF geometry. Table 1 gives an at-a-glance overview of some properties of a range of HFs. The fibers selected are from our internal research (fibers #1,2,4,5,12-14,17) and from the literature.

In order to exploit the full range of novel properties that can be very sensitive to the hole size and arrangement, it is crucial to have accurate techniques for predicting these properties. However, the models developed for conventional fibers cannot generally be applied. HFs exhibit complex transverse index profiles resulting in complex mode field shapes and large index contrast between core and cladding. In addition, the presence of wavelength-scale features introduces a number of challenges for accurate modeling. However, several methods have demonstrated their suitability in modeling different types of HFs [2].

Table 1: Features and properties of selected HFs. Λ is the hole-to-hole pitch, d/Λ is the relative hole size, A_{eff} is the effective mode area, γ is the effective nonlinear coefficient, D is the dispersion and λ_0 is the zero-dispersion wavelength. Note the nonlinear refractive index, n_2, of silica is 2.2×10^{-20} m^2/W. SMF28 is a standard silica fiber. SF57 and SF6 are lead silicate glasses.

No.	glass	Λ (μm)	d/Λ	core size (μm)	A_{eff} at 1.5μm (μm^2)	γ at 1.5μm (W^{-1} km^{-1})	loss at 1.5μm (dB/km)	D at 1.5μm (ps/nm/km)	λ_0 (μm)	comment	Ref
1	silica	12.8	0.06	25[a]	680	0.1[c]					[19]
2	silica	13.5	0.13	25.2[a]	380	0.2[c]					[20]
3	silica	11.5	0.18	28	350	0.3[c]				3-rod core	[24]
4	silica	11.3	0.24	19.9[a]	230	0.4[c]					[20]
5	silica	9.7	0.30	16.5	120[b]	0.7[c]				double-cladding	[23]
6	silica	8.0	0.50	12[a]			0.28	+30	1210		[99]
7	silica	7.5	0.43	11.8[a]	72		1.7				[22]
	SMF28			8.0	90	1.0	0.2	+17	1300		
8	silica	2.6	0.22	4.6[a]			2000	+1 ultraflat	1100		[113]
9	silica	1.5	0.33	2.5[a]	9.6[b]	11	10	-2 ultraflat		hybrid triangular core	[73]
10	silica	1.8	0.60	2.6					840		[103]
11	silica	1.6	0.88	1.7			50		767		[40]
12	silica		large	1.6	2.9	31	40	+100	~800		[27,104]
13	silica		large	1.2	1.5	70	190	-30			[36]
14	silica		large	1.0	1.5	60	300	-350			[32]
15	silica		>0.9	1.0					565		[103]
16	SF6		large	2.6	4.0	200	4.0	+50	1300	$n_2=22\times10^{-20}m^2/W$	[7]
17	SF57		large	1.7	2.6	660	2.6[e]	+88[d]	1280	$n_2=41\times10^{-20}m^2/W$	[11,12]

a) calculated core size = 2Λ-d
b) calculated $A_{eff} = \pi/4\times MFD^2$, where MFD is the mode field diameter
c) calculated according to equation (2)
d) calculated value
e) loss value for 2.0μm core

Images for fiber #5 see Fig. 1b, for fiber #12 see Fig. 1c, for fiber #13 see Fig. 1d, for fiber #17 see Fig. 1e.

3.1. Endless single-mode guidance and second-order cutoff

In standard fibers, the normalized frequency V determines the second-order cutoff between the single-mode and multi-mode guidance. This concept has been applied to HFs and the following formulation was proposed [84]:

$$V = 2\pi\Lambda/\lambda\sqrt{n_{FM}^2 - n_{FSM}^2} \quad (1)$$

where $n_{FM}(\lambda)$ is the wavelength dependent effective index of the fundamental mode (FM) and $n_{FSM}(\lambda)$ is the corresponding effective index of the first cladding mode in the infinitive periodic cladding structure often denoted the fundamental space filling mode (FSM). Mortensen et al. [84] argued that the second-order cutoff occurs for $V^*=\pi$. In contrast to standard fibers, the V parameter of HFs shows an asymptotic behavior in the short wavelength limit [84-88]. As the wavelength decreases, the field becomes more concentrated in the core region and avoids the holes. This raises the effective index of the cladding, which counteracts the explicit dependence of V on the wavelength and so extends the single-mode range. The limiting value of V for $\lambda\rightarrow0$ decreases with decreasing d/Λ [84-87]. Therefore, at sufficient low d/Λ, the V parameter stays below the cutoff value V^* and endless single-mode guidance regardless the wavelength is guaranteed. Calculations using different models have demonstrated that endless single-mode guidance exists for $d/\Lambda<0.406$-0.45 [84,86,87,90]. Mortensen et al. found an empirical expression for the cutoff wavelength λ^*/Λ [84]: $\lambda^*/\Lambda = a\,(d/\Lambda - d^*/\Lambda)^b$, where $a=2.80\pm0.12$, $b=0.89\pm0.02$ and $d^*/\Lambda=0.406$. The latter parameter marks the boundary to endless single-mode guidance. This expression derived from numerical calculations was confirmed experimentally by Folkenberg et al. [91].

3.2. Mode area and nonlinearity

The effective nonlinearity coefficient, γ, can be tailored via the effective mode area, A_{eff}, and the nonlinear refractive index, n_2, by [92]

$$\gamma = 2\pi n_2 / (\lambda A_{\text{eff}}) \quad (2)$$

Simply by scaling the features in the HF profile, the mode area can range over 3 orders of magnitude and thus the effective nonlinearity can be considerably lower or higher compared with standard fibers (Table 1). In addition, the relative hole size determines the effective mode area [18,93]. The larger the hole size, the more confined is the mode in the core region and thus the effective mode area decreases. Large and small mode area HFs differ considerably in their properties as described below.

In large mode area HFs (LMA-HFs), the hole-to-hole pitch Λ is larger than the wavelength ($\Lambda \geq 5\mu m$). For small relative hole sizes $d/\Lambda < 0.4$, they exhibit low nonlinearity and endless single mode guidance (fibers #1-5 in Table 1). This makes LMA-HFs very attractive for delivery and generation of high power laser beams from the ultraviolet to the near-infrared spectral range with high spatial mode quality and without exciting undesired nonlinear effects. In addition, the possibility of using pure silica cores in HFs in contrast to Ge-doped cores in conventional fibers allows the propagation of higher powers without thermo-optical distortions and material damage. However, macro- and microbending losses ultimately limit the mode area that can be utilized in HFs as described below.

At the other extreme, small mode area HFs (SMA-HFs) have features in the wavelength-scale ($\Lambda \leq 3\mu m$) and large relative hole size (fibers #10-17 in Table 1), which gives rise to larger index contrast between core and cladding and thus large numerical aperture (NA) of the fiber. As a result, the mode is more confined to the core region, and thus such fibers exhibit high effective nonlinearity. Silica HFs with up to 70 times higher nonlinearity than standard fibers have been demonstrated [32,36]. The use of compound glass with high nonlinear refractive index allows a further dramatic increase of the effective nonlinearity. Recently, a lead silicate HF with 600 times higher nonlinearity than standard fibers has been demonstrated [11,12]. Due to their small scale features and their large air-filling fraction, the waveguide contribution to the SMA-HF dispersion is considerable, which allows the dispersion to be tailored to suit a range of nonlinear applications. In addition, the birefringence is critically dependent on the symmetry, and so large form birefringence can be achieved in SMA-HFs. In terms of practicality, critical issues in SMA-HFs are confinement loss and propagation loss due to surface roughness as described below. Furthermore, splicing and cleaving to standards fibers is challenging because of the small wavelength-scale cores. However, low splicing losses have recently be achieved by means of intermediate mode area buffer fibers, which have reduced the mode mismatch between the small core highly nonlinear HF and the standard fiber [83].

3.3. Bend loss

Large mode area fibers are susceptible to macro- and microbend loss [17,19-21,85,87,94,95]. The bend loss limits the obtainable mode area at a given wavelength. As in conventional fibers, a long wavelength edge is observed for macrobend loss. However, in contrast to conventional fibers, a short wavelength edge appears as a result of the decreasing index difference between core and cladding for $\lambda \rightarrow 0$. The critical bend radius is proportional to Λ^3/λ^2 [17,85,94]. The long and short wavelength edge determine the useful spectral window of the HF. Large hole sizes result in broad windows, whereas the pitch Λ determines the center position of the window [94]. Baggett et al. [19,20] studied experimentally and theoretically the impact of cladding geometry and angular orientation of the HF on the bend loss and compared the results with conventional fibers. They observed that for a given mode area HFs demonstrate similar bend loss values at 1550nm compared with conventional fibers. To increase the useful mode area, Mortensen et al. [21] developed a 3-rod core HF that demonstrates less bend loss for a fixed mode field diameter.

3.4. Propagation loss

Since pure silica has a lower Rayleigh scattering loss than Ge-doped silica [96], pure silica HFs have the potential for lower loss than standard Ge-doped fibers. In addition, the use of a single material in HFs eliminates losses that arise in conventional fibers due to viscosity mismatch between the core and the cladding material [97]. The ultimate loss limit for pure silica has been found to be 0.14dB/km [98], whereas standard fibers exhibit 0.20dB/km. To date the lowest loss obtained in HFs has been 0.28dB/km [99]. The OH absorption loss contribution in this HF is comparable with conventional fibers. The excess loss of the HF originates from imperfections on the holes and enhanced Rayleigh scattering due to surface roughness. Further improvements of the fabrication are anticipated to result ultimately in losses

near the limit for pure silica. Hollow-core photonic bandgap fibers in principal promise even lower losses, because the light travels predominantly in the hollow core. However, the high sensitivity of the bandgap to structural fluctuations makes great demands on the fabrication to achieve such low losses [4]. To date the best reported propagation loss in hollow-core photonic bandgap fiber is 13dB/km [6].

In general, SMA-HFs demonstrate higher losses than LMA-HFs since reducing the core diameter to dimensions comparable to the wavelength of light increases the fiber loss for two principle reasons. In SMA-HFs, confinement loss can have a significant impact [100]. The modes of single-material HFs are leaky because the core refractive index is the same as that beyond the finite holey cladding, and for some designs, this can lead to significant confinement loss. In SMA-HFs, the mode can see over the finite cladding region unless many rings of holes are used. Increasing the number of rings always decreases the confinement loss, but it also increases drastically the fabrication labor and decreases the robustness of the fiber. Fortunately, a modest increase in the structure scale can lead to dramatic improvements in the confinement of the mode without compromising the achievable effective nonlinearity significantly. Furthermore, the effective mode area and fiber dispersion are independent of the number of rings for HFs with two or more rings [100]. In addition to confinement loss, the effect of surface roughness at the air/glass boundary becomes more significant, since the light interacts much more with the air/glass boundaries near the core. This can increase the loss as a result of enhanced scattering [99,101,102]. To date small core highly nonlinear HFs with losses down to ~50dB/km have been achieved. Since for highly nonlinear fibers, only short lengths (<10m) are typically required, loss values of the order of 100dB/km can be readily tolerated.

Highly nonlinear compound glass HFs exhibit higher losses than their silica counterparts due to higher losses of the bulk glasses itself and due to the fact that the fabrication technology of such fibers is still at an early stage of development. To date typically losses are 3-5dB/m [7,8,10,12,13]. However, the much higher nonlinearities of these fibers decrease the required fiber lengths to ≤1m, and thus loss values below 1dB/m can be tolerated.

3.5. Fiber dispersion

In SMA-HFs, the waveguide contribution to the chromatic fiber dispersion can be large, in particular for small Λ and large d/Λ. This allows engineering of the dispersion to suit the demands for a range of applications. By decreasing the pitch Λ and the increasing the relative hole size d/Λ, the zero dispersion wavelength can be shifted to shorter wavelengths down to 560nm (Table 1) [103]. In general, a drastic shift is observed for Λ=1-2μm and $d/\Lambda \geq 0.5$ [40,103,104]. The extension of anomalous dispersion down to 550nm has made soliton generation and propagation in the near-infrared and visible spectrum possible. Shifting the zero-dispersion wavelength to regimes where there are convenient high-power fs laser sources (Ti:sapphire at 800nm, Yb-fiber and Nd:YAG at 1060nm) also allows the development of efficient supercontinuum sources, which are attractive for a range of applications (see section 4). On the other hand, wavelength converters based on cross-phase modulation [32] and optical thresholding devices [27] based on self-phase-modulation require small normal dispersion to minimize coherence degradation. In addition, parametric oscillators and wavelength converters based on four-wave-mixing [33,36] require small normal dispersion to achieve efficient phase matching. The impact of fiber dispersion on pulse propagation, supercontinuum spectra and four-wave-mixing was experimentally studied in Refs. [41,105,106] and theoretically modeled in Refs. [107,108]. For dispersion compensation of standard fibers, a large normal dispersion is needed at 1550nm [109,110]. In addition to the value, the slope of the dispersion is important. Ultraflat dispersion at the wavelength range of interest enhances the useful spectral bandwidth of nonlinear devices [48,73,111-113]. Several methods have been developed to design HFs with ultraflat dispersion of a certain value and for a certain wavelength range. For example, ultraflat dispersion is obtained for fibers with Λ=2-3μm and d/Λ=0.2-0.3 for 1300-1800nm [112,113]. Unfortunately, such fibers have large confinement loss unless more than 10 rings of holes are used (fiber #8 in Table 1) [113]. To overcome this difficulty, improved designs were proposed including rings of increasing hole size [114,115] and hybrid triangular cores (fiber #9 in Table 1) [73].

The large contribution of waveguide dispersion possible in HFs is in particular remarkable for compound glass HFs. Compound glasses with large refractive index exhibit a large normal material dispersion at 1550nm. However, the SMA-HFs design with small cores and large air-filling fractions allows to overcome this material dispersion and to achieve anomalous dispersion at 1550nm (fibers #16&17 in Table 1) [7,12].

3.6. Birefringence

SMA-HFs can exhibit large form birefringence, which is of interest for stable operation of nonlinear devices. In particular for small Λ and large d/Λ, any slight deviation from symmetry result in considerable birefringence. Highly

birefringent HFs have been achieved using different hole sizes and/or asymmetric hole arrangement [27,69,70,74,77-79]. In this way, beat lengths down to 0.3mm (birefringence up to 10^{-3}) have been achieved [69,70]. On the other side, LMA-HFs can have very low birefringence. Ritari et al. [80] have demonstrated that excellent cladding symmetry resulted in a very large beat length of 21m. In contrast to conventional fibers, the birefringence of HFs increases towards longer wavelengths as a result of the strong wavelength dependence of the cladding refractive index, which raises the index difference between core and cladding [116].

4. DEVICE APPLICATIONS

4.1. Overview

According to their large variety in properties, HFs are attractive for wide range of applications. For example, LMA-HFs are attractive for delivery and generation of high power laser beams. In passive devices, error-free transmission of data streams over several km fiber length have been demonstrated [22,37]. As for active devices, double-clad LMA-HFs allow effective cladding pumping, which results in high power laser generation [23-25].

At the other extreme, SMA-HFs can have high values of nonlinearity per unit length (see section 3.2) and thus nonlinear optical devices based on them can be much shorter in length, and/or operate at lower power levels than devices based on conventional fiber types. HFs thus promise practical nonlinear fiber devices for use within a variety of application areas including future high capacity optical communication systems, medicine, metrology and spectroscopy. To date, for silica HFs, a range of nonlinear devices have already been demonstrated including:

- regeneration and thresholding devices [26,27] and pulse compression devices [28] based on self-phase-modulation (SPM)
- nonlinear optical loop mirror switches [29], nonlinear optical loop mirror demultiplexers [30] and wavelength converters [31,32] based on cross-phase-modulation (XPM)
- parametric oscillators [33,34], parametric amplifiers [35] and wavelength converters [36,37] based on four-wave-mixing (FWM)
- wavelength converters [38,39] based on harmonic generation
- supercontinuum generation [40-49] for DWDM transmitters [50], optical frequency metrology [51], optical coherence tomography [52], and spectroscopy [53]
- soliton generation [54] and propagation including self-soliton-frequency shift [55-58]
- Raman lasers and amplifiers [59,60] and Brillouin lasers [61]

As for highly nonlinear compound glass HFs, Raman soliton generation [11,12] and supercontinuum generation [8,62] has been reported for lead-silicate fibers. A selection of nonlinear device demonstrators is described in section 4.2. To date most HF device work has concentrated on the use of small core silica HFs, which have around 50 times the nonlinearity of standard fibers. This reduces the typical power length product requirements of such devices to the 10W·m level. The development of compound glass HFs with several hundred times the nonlinearity of standard fibers should ultimately allow sub-meter/sub-Watt devices to be realized.

Since the dispersion of HFs can be tailored over a wide range of values, HFs promise devices for dispersion control. Dispersion compensation has been demonstrated for soliton and Raman lasers [117-119]. HFs with very small cores and large air-filling fraction are of interest for short-length dispersion compensation at 1550nm, since they exhibit very high normal dispersion at 1550nm [109,110].

HFs with very small core and large air-filling fraction are also of interest for evanescent field devices. In such fibers, a very large fraction of the mode field can be located within the air holes [120]. This allows strong interaction of light with gases or liquids in the holes via evanescent field effects, which can be utilized for sensor devices [121]. The easy fabrication of multi-core HFs has been utilized in two-core couplers [75] and Doppler difference velocimeters [76].

HFs can be readily doped with rare-earth ions and thus they are also of great interest for active devices. Different erbium- and ytterbium-doped HF lasers and amplifiers have already been demonstrated [23-25,68-72,83] and a selection of devices is described in section 4.3. The combination of dispersion, birefringence, nonlinearity and mode confinement control together with amplification and lasing promises new types of active devices.

4.2. Nonlinear devices

Early device demonstrations of a nonlinear HF were reported in 2001 and 2002 and concerned 2R regeneration and optical thresholding at 1550nm [26,27]. The regeneration technique employed makes use of spectral broadening of a

pulse due to SPM. The HF that was used for this demonstration is shown in Fig. 1c and the properties are listed in Table 1, fiber #12. A filter is set with its peak transmission wavelength offset from the central wavelength (1553nm) of an incoming data stream such that low power pulses propagating within the HF generate little SPM and are thus largely rejected by the filter. By contrast, higher power pulses generate appreciable SPM (Fig. 2) such that significant power is now generated at wavelengths within the filter passband. These spectral components are then transmitted by the filter. It can be shown that around some critical input pulse intensity the intensity of the output pulses becomes independent of the input intensity, providing the input intensity is large enough to produce sufficient SPM. Such a nonlinear response can be used as a means to provide 2R regeneration since noisy zero bits are suppressed and noisy one bits have their intensity equalized. The reshaping part of the 2R process is obtained through the narrowband filtering process itself assuming that a filter with an appropriate phase and amplitude response matched to the incoming pulse response is used. A plot of a typical nonlinear transmission response for such a switch is shown in Fig. 2 (Left). The S-shaped transmission characteristics are just as required for 2R regeneration and optical thresholding applications. In this particular instance the length of the HF used was 8.7m, and the operating switching power was ~2W. This particular switch was used as an optical thresholder and allowed error-free performance with reduced power penalty relative to a simple linear receiver. In the earliest experiment of this approach regenerative operation of a 3.3m switch was reported with a pulse operating power of 16 W. Note that in order to get the most stable operation of the filtered SPM schemes it is best to use HFs with normal rather anomalous dispersion since coherence degradation is known to result in amplitude noise when anomalously dispersive fiber is used [122].

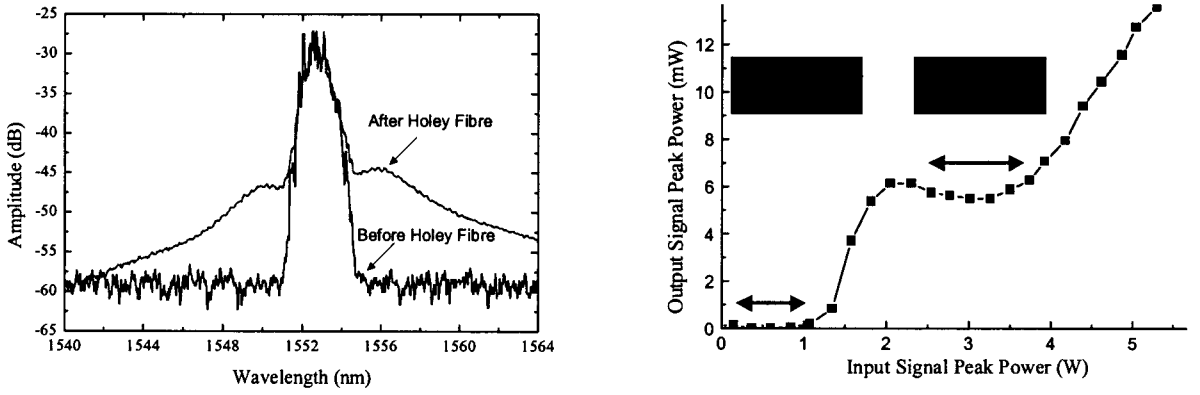

Fig. 2. Optical thresholding device using highly nonlinear silica HF (#12 in Table 1, image see Fig. 1c) and mode locked erbium fiber ring laser operating at 1553nm and generating 2.5ps soliton pulses: (Left) SPM broadened spectra, (Right) power transmission characteristics of the HF switch as a function of the input peak power.

It is also possible to extend the spectral broadening followed by offset narrowband filtering technique to work using XPM, and thereby to allow for signal wavelength conversion at around 1550nm [31,32]. In this instance a continuous wave probe beam, or indeed multiple probe beams, are launched into the HF along with the data signal. XPM between the control signal and the CW beams results in chirping of the CW laser beam where these beams overlap temporally within the fiber. The frequency chirping of the CW laser beam can then be converted to a frequency converted signal by passing this chirped signal through a narrowband filter to eliminate the residual unchirped CW signal and the original data signal. In an early experiment [31], a nonlinear HF with anomalous dispersion at 1550nm was used (Fig. 1c, fiber #12 in Table 1), which resulted in amplitude noise on the converted signals due to coherence degradation. In a later experiment [32], a nonlinear HF with normal dispersion at 1550nm was used (fiber #14 in Table 1). Fig. 3 (Left) shows the results of an experiment in which 3 CW probe beams in the range of 1530-1580nm are propagated with a relatively intense data signal pulses of 2.5ps at 1552nm within just 5.8m fiber, resulting in the generation of 3 wavelength converted signals. Fig. 3 (Right) also shows the measured temporal width of the wavelength converted pulses as a function of probe beam wavelength. The pulse widths of the converted pulses were observed to be almost constant at ~11ps over a wavelength range of ~15nm. The normal dispersion of the HF eliminated coherence degradation effects, and thus error-free, almost penalty-free wavelength conversion performance was obtained.

An alternative, and more flexible approach for wavelength conversion, is based on FWM of a signal beam at a fixed wavelength of 1550nm with a pump wavelength in the range 1530-1580nm [36]. Highly efficient, broadband wavelength conversion requires high nonlinearity, low dispersion, low dispersion slope, and a short fiber length so as to reduce the phase mismatch between interacting waves. These demands were fulfilled by using a highly nonlinear HF

with small normal dispersion at 1550nm (Fig. 1d, fiber #13 in Table 1). The reduction of stimulated Brillouin scattering (SBS) effects is a key issue in such devices and is required to suppress SBS-induced pump power loss [123]. A high SBS threshold was obtained due to broadening of the Brillouin lineshape through structural variation along the fiber length [61]. The results of a FWM-based wavelength conversion experiment employing 15m HF are shown in Fig. 4. The wavelength of the initial signal and pump beams are 1550 and 1547nm, respectively. In the output spectrum, a strong FWM wavelength converted signal is clearly evident at 1544nm despite the short fiber length used and both second- and third-order idler beams are also observable. After the HF, a narrowband filter was used to efficiently suppress the input signal and pump beams and to pick out the wavelength converted signal. Fig. 4 (Left) shows the measured conversion efficiency, which is defined as the ratio of output wavelength-converted signal power to the input signal power. A maximum conversion efficiency of –16dB was achieved over a 3dB bandwidth of ~10nm. Since the fiber had normal dispersion, no modulation-instability-induced intensity noise was observed.

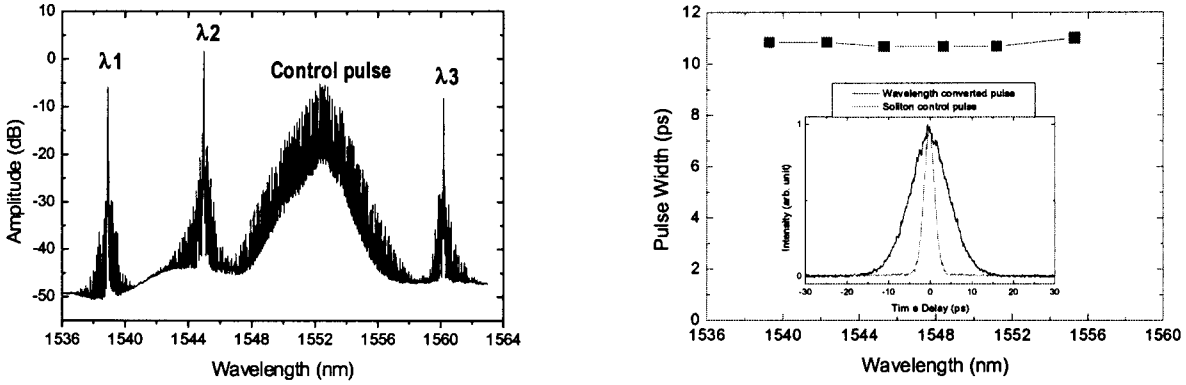

Fig. 3. XPM-based wavelength converter using highly nonlinear silica HF (#14 in Table 1). The control pulses were generated form a mode locked erbium fiber ring laser operating at 1552nm and generating 2.5ps soliton pulses. The probe beams were generated from tunable cw external cavity lasers operating in the range 1530-1580nm: (Left) Measured optical spectrum of the three wavelength converted signals and of the control pulses after the HF, (Right) FWHM of the wavelength converted pulses as a function of the probe beam wavelength for the case of wavelength conversion of a single channel. The inset shows the SHG autocorrelation traces of the wavelength converted pulses at 1545nm, and the input pulses.

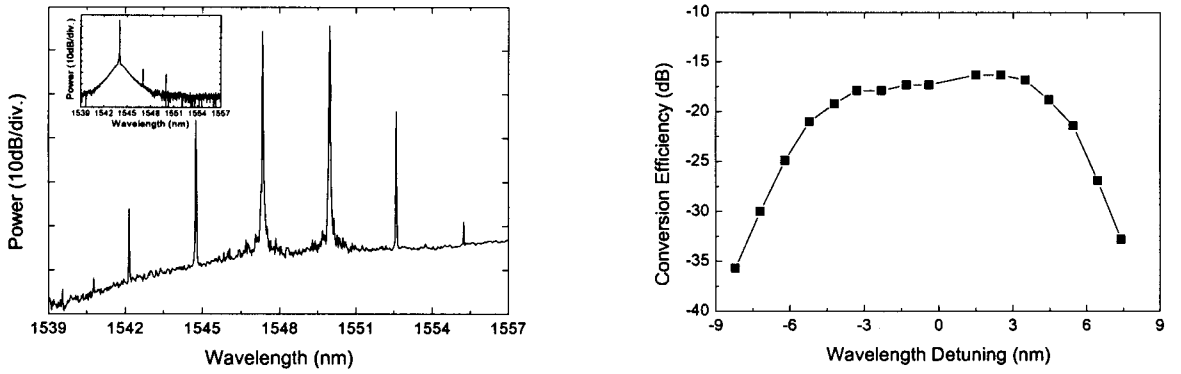

Fig. 4. FWM-based wavelength converter using highly nonlinear silica HF (#13 in Table 1, image see Fig. 1d) and tunable cw external cavity lasers operating in the range 1530-1580nm: (Left) output FWM spectrum after the HF: wavelength converted signal (~1545nm), pump (~1552nm), input signal (~1549nm) and idler with filtered spectrum shown inset, (Right) conversion efficiency as function of detuning relative to a fixed wavelength of 1550nm.

Supercontinuum generation offers the development of broadband coherent optical sources for DWDM transmitters at 1550nm by generating short pulses with a broad spectral content which can be efficiently sliced to provide multiple short pulse WDM channels [50]. Efficient broadening and subsequent slicing has been achieved with 20m length of the highly nonlinear HF (Fig. 1d, fiber #13 in Table 1) that have been used for the wavelength conversion experiment described above and using just 240mW input power. After propagation through the HF, the soliton pulses broadened from 3nm to 17nm due to development of self-phase modulation in the presence of the normal dispersion of the HF. The

broadened spectrum was then sliced using an arrayed waveguide grating (AWG) providing a 3dB bandwidth of 0.5nm for each of its channels. The channel separation was 100GHz. Fig. 5 shows the optical spectra before the HF, after the HF and at the output of one of the AWG channels. Deep 10GHz longitudinal modes are clearly resolved in all spectral measurements indicating that the phase coherence properties of the original pulses are maintained. All channels gave error-free operation with no significant power penalty relative to each other.

The potential of highly nonlinear compound glass HFs for compact nonlinear devices operating at low pump powers was demonstrated for Raman soliton generation in a lead silicate HF with ten times higher nonlinearity than highly nonlinear silica HFs [11,12]. Fig. 6 shows self-frequency-shifting of soliton pulses in 2.2m of HF as a function of input energy. Note that the effective fiber length was just 0.47m. For 90pJ input energy (~110mW average power), the original pulses were shifted by ~80nm. For autocorrelation measurements, a shorter fiber length of 0.37m (effective length of 0.26m) was used to ensure that the effective nonlinear interaction length is similar to the actual fiber length. In this instance, a similar wavelength shift was found for a given input energy. The autocorrelation trace of pulses at the HF output showed a pulse width of ~190fs, which indicates 10fold pulse compression.

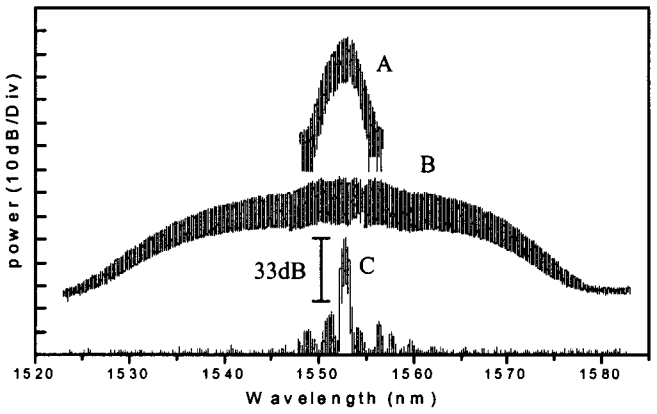

Fig. 5. Spectral broadening and subsequent slicing using highly nonlinear silica HF (#13 in Table 1, image see Fig. 1d) and mode locked erbium fiber ring laser operating at 1556nm and generating 2.1ps soliton pulses. The average power of the pulses launched into the HF was ~240mW. Input (A), supercontinuum (B) and one of the filtered spectrum (C).

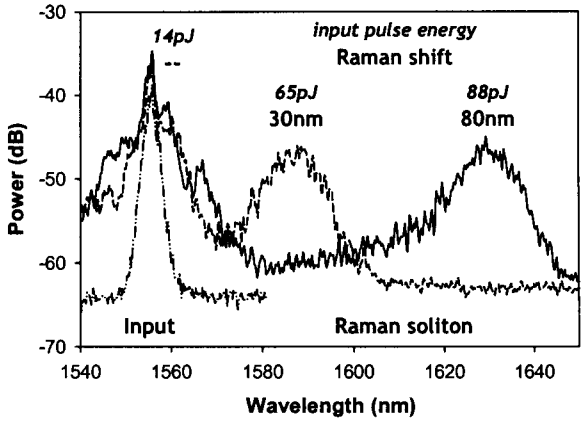

Fig. 6. Raman soliton generation using small core highly nonlinear lead-silicate HF (#17 in Table 1, image see Fig. 1e) and a mode locked erbium fiber ring laser operating at 1552nm and generating ~2ps soliton pulses: Traces of the Raman soliton spectra at the output of the HF for various levels of input pulse energies.

4.3. Active devices

HF technology offers interesting properties for the development of active fibers and devices. For example, all-glass double-clad fibers with large mode area and single-mode guidance allow for cladding-pumped high power laser generation with relatively tight pump radiation confinement and single transverse mode laser operation [23-25]. Here we review the first demonstration of this fiber type [23]. The fiber has an Yb^{3+}-doped core surrounded by an inner cladding consisting of 5 rings of small holes (Fig. 1b, fiber #5 in Table 1). The inner cladding NA was measured to be 0.3. Two rings of larger holes define the outer cladding. Note that the core is offset, which breaks the cladding symmetry, and hence enhances pump absorption. A cladding-pumped laser was realized using a low brightness 915nm fiber-coupled laser diode. Using a Fabry-Perot cavity, average powers in excess of 1W were achieved in 7.5m fiber length, with a measured slope efficiency of 70%. Note that in addition to optical isolating the inner structure from the external environment, the air cladding also provides thermal isolation. Although this might be expected to lead to thermal problems, no such issues were encountered in these experiments even at a multi-Watt pump levels. Both Q-switched and mode-locked operation were demonstrated in this cladding pumped HF laser. In the mode-locking experiments, fundamental mode-locking was obtained over a wavelength tuning range in excess of 60nm. The pulse duration was estimated to ~100ps. An output power of more than 500mW was achieved for a pump power of 1.33W. The ultimate advantages of double-clad HFs relative to polymer coated dual clad fibers are that they allow for all-glass structures, with inner cladding NAs in excess of 0.5 and good pump/mode mixing. The all-glass structure increases the power handling capability that can be used in the fiber.

At the other extreme, rare-earth doped small-core high-NA HF designs allow for tight pump and signal mode confinement, thereby allowing for high small-signal gain efficiencies and low laser thresholds. Recently, a fully fiberized erbium doped HF ring laser based on 4.5m of aluminosilicate-erbium doped HF has been demonstrated [83]. The laser threshold was just 0.48mW of 980nm pump at the optimum operating wavelength of 1550nm. This ultra-low threshold, which is 5-10 times lower than that for conventional erbium-doped fiber lasers, results form the tight spatial confinement and strong overlap of the erbium dopant and the pump/signal optical field [71]. The laser had a tuning range of 104nm which is comparable to the best ever achieved with conventional erbium fibers and limited primarily by the bandwidth of the tunable filters used.

The combination of high nonlinearity and anomalous dispersion at short wavelengths allows the possibility of extending soliton source concepts to Yb-doped fiber amplifiers operating around 1μm. In this way, a continuously tunable fs soliton source has been realized [70]. This source is seeded by a diode-pumped 1030nm Yb-doped silica fiber laser, and relies on self-soliton-frequency-shift (SSFS) effects in an Yb-doped HF amplifier. The fiber used in these experiments is shown in Fig. 1f. This fiber is single mode for all wavelengths considered here, and has an effective mode area of just 2.5μm^2 at 1550nm. The mode-locked seed laser produces pulses at 1060nm with a positive linear chirp, which are launched into the Yb-doped HF amplifier, together with a 966nm pump beam from a diode laser to control the gain. Because of the amplification and nonlinear evolution of the pulses as they pass through the amplifier, Raman solitons form and are continuously wavelength shifted via the SSFS. Since the nonlinear evolution of the pulses depends on the pulse peak power, the wavelength of the Raman solitons at the amplifier output can be tuned by varying the gain in the amplifier. Using ~5m of amplifier fiber, single-color soliton output pulses have been wavelength tuned from 1060-1330nm (Fig. 7). The final central wavelength of the pulses varies in an almost linear fashion with the level of incident pump power. Note that the maximum wavelength shift of the Raman soliton increases with the length of fiber used, and is ultimately limited by the absorption of silica near 2.3mm.

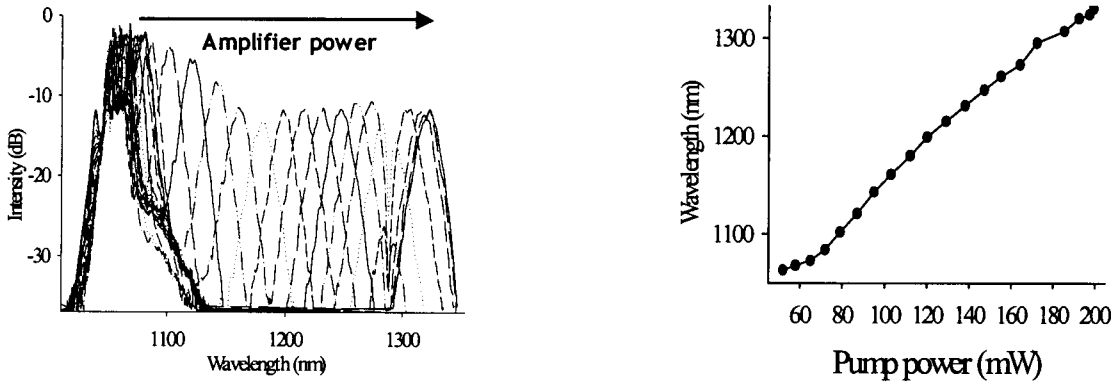

Fig. 7. Tunable single-color solitons using small-core high-NA Yb-doped HF amplifier (image see Fig. 1f), a fs Yb-doped fiber laser for seeding and a laser diode at 966nm for pumping: (Left) superimposed spectra of the solitons shifted to progressively longer wavelengths, (Right) plot of the soliton wavelength versus amplifier incident pump power.

5. Conclusions

The field of HFs has developed rapidly, and a wide range of robust, low-loss index-guiding silica HFs can now be routinely fabricated. Based on the novel guiding regimes and unique features of HFs, numerous device applications with tailor-made optical properties have been demonstrated for use in telecommunications, medicine, metrology and beyond, which shows that the HF technology becomes increasingly mature. In recent years, the concept of HF technology has been extended to highly nonlinear compound glass HFs. The fabrication of HFs with different structures and using different glass types highlights the large versatility of the HF concept. Early device demonstrators using lead silicate HFs promise the development of devices with properties not possible with silica HFs.

References

1. J. C. Knight, T.A. Birks, P.S.J. Russell, D.M. Atkin, "All-silica single-mode optical fiber with photonic crystal cladding", *Opt. Lett.* **21**, pp. 484-485, 1996
2. T.M. Monro, D.J. Richardson, "Holey optical fibres: Fundamental properties and device applications", *C. R. Phys.* **4**, pp. 175-186, 2003
3. J.C. Knight, "Photonic crystal fibres", *Nature* **424**, pp. 847-851, 2003

4. P. Russell, "Photonic crystal fibers", *Science* **299**, pp. 358-362, 2003
5. R.F. Cregan, B.J. Mangan, J.C. Knight, T.A. Birks, P.S. J. Russell, P.J. Roberts, D.C. Allan, "Single-mode photonic band gap guidance of light in air", *Nature* **285**, pp.1537-1539, 1999
6. C.M. Smith, N. Ventkataraman, M.T. Gallagher, D. Muller, J.A. West, N.F. Borelli, D.C. Allan, K.W. Koch, "Low-loss hollow-core silica/air photonic bandgap fibre", *Nature* **424**, pp. 657-659, 2003
7. V.V.R.K. Kumar, A.K. George, W.H. Reeves, J.C. Knight, P.S.J. Russell, "Extruded soft glass photonic crystal fiber for ultrabroadband supercontinuum generation", *Opt. Express* **10**, pp. 1520-1525, 2002
8. V.V.R.K. Kumar, A.K. George, J.C. Knight, P.S.J. Russell, "Tellurite photonic crystal fiber", *Opt. Express* **11**, pp. 2641-2645, 2003
9. K.M. Kiang, K. Frampton, T.M. Monro, R. Moore, J. Trucknott, D.W. Hewak, D.J. Richardson, "Extruded singlemode non-silica glass holey optical fibres", *Electron. Lett.* **38**, pp. 546-547, 2002
10. T.M. Monro, K.M. Kiang, J.H. Lee, K. Frampton, Z. Yusoff, R. Moore, J. Trucknott, D.W. Hewak, H.N. Rutt, D.J. Richardson, "High nonlinearity extruded single-mode holey optical fibers", *Proc. Optical Fiber Communications Conference (OFC'2002),* Anaheim, California, 2002, postdeadline paper FA1-1
11. P. Petropoulos, T.M. Monro, H. Ebendorff-Heidepriem, K. Frampton, R.C. Morre, H.N. Rutt, D.J. Richardson, "Soliton-self-frequency-shift effects and pulse compression in anomalously dispersive high nonlinearity lead silicate holey fiber", *Proc. Optical Fiber Communications Conference (OFC'2003),* Atlanta, Georgia, 2003, postdeadline paper PD03
12. P. Petropoulos, H. Ebendorff-Heidepriem, V. Finazzi, R.C. Moore, K. Frampton, D.J. Richardson, T.M. Monro, "Highly nonlinear and anomalously dispersive lead silicate glass holey fibers", *Opt. Express* **11**, pp. 3568-3573, 2003
13. H. Ebendorff-Heidepriem, P. Petropoulos, V. Finazzi, K. Frampton, R.C. Moore, D.J. Richardson, T.M. Monro, "Highly nonlinear bismuth-oxide-based glass holey fiber, *Proc. Optical Fiber Communications Conference (OFC'2004),* Los Angeles, California, 2004, paper ThA4
14. M.A. van Eijkelenborg, M.C.J. Lange, A. Argyros, J. Zagari, S. Manos, N.A. Issa, S. Fleming, R.C. McPhedran, C.M. de Sterke, N.A.P. Nicorovici, "Microstructured polymer optical fibre", *Opt. Express* **9**, pp. 319-327, 2001
15. X. Feng, T.M. Monro, P. Petropoulos, V. Finazzi, D.W. Hewak, "Solid microstructured optical fiber", *Opt. Express* **11**, pp. 2225-2230, 2003
16. T.M. Monro, P.J. Bennett, N.G.R. Broderick, D.J. Richardson, "Holey fibers with random cladding distributions", *Opt. Lett.* **25**, pp. 206-208, 2000
17. J.C. Knight, T.A. Birks, R.F. Cregan, P.S.J. Russell, J.-P. de Sandro, "Large mode area photonic crystal fibre", *Electron. Lett.* **34**, pp. 1347-1348, 1998
18. T. M. Monro, D.J. Richardson, N.G.R. Broderick, P.J. Bennett, "Holey optical fibers: an efficient modal model", *J. Lightwave Technol.* **17**, pp. 1093-1102, 1999
19. J.C. Baggett, T.M. Monro, K. Furusawa, D.J. Richardson, "Comparative study of large-mode holey and conventional fibers", *Opt. Lett.* **26**, pp. 1045-1047, 2001
20. J.C. Baggett, T.M. Monro, K. Furusawa, V. Finazzi, D.J. Richardson, "Understanding bending losses in holey optical fibers", *Opt. Commun.* **227**, pp. 317-335, 2003
21. N.A. Mortensen, M.D. Nielsen, J.R. Folkenberg, A. Petersson, H.R. Simonson, "Improved large-mode-area endlessly single-mode photonic crystal fibers", *Opt. Lett.* **28**, pp. 393-395, 2003
22. B. Zsigri, C. Peucheret, M.D. Nielsen, P. Jeppesen, "Transmission over 5.6km large effective area and low-loss (1.7dB/km) photonic crystal fibre", *Electron. Lett.* **39**, pp. 796-798, 2003
23. K. Furusawa, A. Malinowski, J.H.V. Price, T.M. Monro, J.K. Sahu, J. Nilsson, D.J. Richardson, "Cladding pumped ytterbium-doped fiber laser with holey inner and outer cladding", *Opt. Express* **9**, pp. 714-720, 2001
24. J.Limpert, T. Schreiber, S. Nolte, H. Zellmer, A. Tunnermann, R. Iliew, F. Lederer, J. Broeng, G. Vienne, A. Petersson, C. Jacobsen, "High-power air-clad large-mode-area photonic crystal fiber laser", *Opt. Express* **11**, pp. 818-823, 2003
25. W.J. Wadsworth, R.M. Percival, G. Bowmans, J.C. Knight, P.S.J. Russell, "High power air-clad photonic crystal fibre laser", *Opt. Express* **11**, pp. 48-53, 2003
26. P. Petropoulos, M. Monro, W. Belardi, K. Furusawa, J.H. Lee, D.J. Richardson, "2R-regenerative all-optical switch based on a highly nonlinear holey fiber", *Opt. Lett.* **26**, pp. 1233-1235, 2001
27. J.H. Lee, P.C. Teh, Z. Yusoff, M. Ibsen, W. Belardi, T.M. Monro, D.J. Richardson, "A holey fiber-based nonlinear thresholding device for optical CDMA receiver performance enhancement", *IEEE Photon. Technol. Lett.* **14**, pp. 876-878, 2002
28. S. Lako, J. Seres, P. Apai, J. Balazs, R.S. Windeler, R. Szipocs, "Pulse compression of nanojoule pulses in the visible using microstructure optical fiber and dispersion compensation", *Appl. Phys. B* **76**, pp. 267-275, 2003
29. J.E. Sharping, M. Fiorentino, P. Kumar, R. S. Windeler, "All-optical switch based on cross-phase modulation in microstructure fiber", *IEEE Photon. Technol. Lett.* **14**, pp. 77-79, 2002
30. A.I. Siahlo, L.K. Oxenlowe, K.S. Berg, A.T. Clausen, P.A. Andersen, C. Peucheret, A. Tersigni, P. Jeppesen, K.P. Hansen, J.R. Folkenberg, "A high-speed demultiplexer based on a nonlinear optical loop mirror with a photonic crystal fiber", *IEEE Photon. Technol. Lett.* **15**, pp. 1147-1149, 2003
31. J.H. Lee, Z. Yusoff, W. Belardi, M. Ibsen, T.M. Monro, B. Thomsen, D.J. Richardson, "A holey fiber based WDM wavelength converter incorporating an apodized fiber Bragg grating filter", *Proc. Conference on Lasers and Electro-Optics (CLEO'2002),* Long Beach, 2002, postdeadline paper CPDB5

32. J.H. Lee, P.C. Teh, W. Belardi, M. Ibsen, T.M. Monro, D.J. Richardson, "A tunable WDM wavelength converter based on cross-phase modulation effects in normal dispersion holey fiber", *IEEE Photon. Technol. Lett.* **15**, pp. 437-439, 2003
33. J.E. Sharping, M. Fiorentino, P. Kumar, R.S. Windeler, "Optical parametric oscillator based on four-wave mixing in microstructure fiber", *Opt. Lett.* **27**, pp. 1675-1677, 2002
34. J. Lasri, P. Devgan, R. Tang, J.E. Sharping, P. Kumar, "A microstructure-fiber-based 10-GHz synchronized tunable optical parametric oscillator in the 1550-nm regime", *IEEE Photon. Technol. Lett.* **15**, pp. 1058-1060, 2003
35. R. Tang, J. Lasri, P. Devgan, J.E. Sharping, P. Kumar, "Microstructure-fibre-based optical parametric amplifier with gain slope of ~200dB/W/km in the telecom range", *Electron. Lett.* **39**, pp. 195-196, 2003
36. J.H. Lee, W. Belardi, K. Furusawa, P. Petropoulos, Z. Yusoff, T.M. Monro, D.J. Richardson, "Four-wave-mixing based 10-Gb/s tunable wavelength conversion using a holey fiber with a high SBS threshold.", *IEEE Photon. Technol. Lett.* **15**, pp. 440-442, 2003
37. C. Peucheret, B. Zsigri, P.A. Andersen, K.S. Berg, A. Tersigni, P. Jeppesen, K.P. Hansen, M D. Nielsen, "40Gbit/s transmission over photonic crystal fibre using mid-span spectral inversion in highly nonlinear photonic crystal fibre", *Electron. Lett.* **39**, pp. 919-921, 2003
38. F. Omenetto, A. Efimov, A.J. Taylor, J.C. Knight, W.J. Wadsworth, P.S.J. Russell, "Polarization dependent harmonic generation in microstructured fibers", *Opt. Express* **11**, pp. 61-67, 2003
39. A. Efimov, A.J. Taylor, F. Omenetto, J.C. Knight, W.J. Wadsworth, P.S.J. Russell, "Phase-matched third harmonic generation in microstructured fibers", *Opt. Express* **11**, pp. 2567-2576, 2003
40. J.K. Ranka, R.S. Windeler, A.J. Stentz, "Visible continuum generation in air-silica microstructure optical fibers with anomalous dispersion at 800nm", *Opt. Lett.* **25**, pp. 25-27, 2000
41. W.J. Wadsworth, A. Ortigosa-Blanch, J.C. Knight, T.A. Birks, T.-P..M. Man, P.S.J. Russell, "Supercontinuum generation in photonic crystal fibers and optical fiber tapers: a novel light source", *J. Opt. Soc. Amer. B* **19**, pp. 2148-2155, 2002
42. S. Coen, A.H.L. Chau, R. Leonhardt, J.D. Harvey, J.C. Knight, W.J. Wadsworth, P.S.J. Russell, "Supercontinuum generation by stimulated Raman scattering and parametric four-wave-mixing in photonic crystal fibers", *J. Opt. Soc. Amer. B* **19**, pp. 753-764, 2002
43. A. Ortigosa-Blanch, J.C. Knight, P.S.J. Russell, "Pulse breaking and supercontinuum generation with 200-fs pump pulses in photonic crystal fibers", *J. Opt. Soc. Amer. B* **19**, pp. 2567-2572, 2002
44. P.A. Champert, S.V. Popov, J.R. Taylor, "Generation of multiwatt, broadband continua in holey fibers", *Opt. Lett.* **27**, pp. 122-124, 2002
45. J.M. Dudley, L. Provino, N. Grossard, H. Maillotte, R.S. Windeler, B.J. Eggleton, S. Coen, "Supercontinuum generation in air-silica microstructured fibers with nanosecond and femtosecond pulse pumping", *J. Opt. Soc. Amer. B* **19**, pp. 765-771, 2002
46. G.E. Town, F. Funaba, T. Ryan, K. Lyytikainen, "Optical supercontinuum generation from nanosecond pump pulses in an irregularly microstructured air-silica optical fiber", *Appl. Phys. B* **77**, pp. 235-238, 2003
47. T. Schreiber, J. Limpert, H. Zellmer, A. Tunnermann, K.P. Hansen, "High average power supercontinuum generation in photonic crystal fibers", *Opt. Commun.* **228**, pp. 71-78, 2003
48. T. Yamamoto, H. Kubota, S. Kawanishi, M. Tanaka, S. Yamaguchi, "Supercontinuum generation at 1.55μm in a dispersion-flattened polarization-maintaining photonic crystal fiber", *Opt. Express* **11**, pp. 1537-1540, 2003
49. M. Lehtonen, G. Genty, H. Ludvigsen, M. Kailova, "Supercontinuum generation in a highly birefringent microstructured fiber", *Appl. Phys. Lett.* **82**, pp. 2197-2199, 2003
50. Z. Yusoff, P. Teh, P. Petropoulos, K. Furusawa, W. Belardi, T.M. Monro, D. Richardson, "24 channels x 10GHz spectrally sliced pulse source based on spectral broadening in a highly nonlinear holey fiber", *Proc. Optical Fiber Communications Conference (OFC'2003)*, Atlanta, Georgia, 2003, paper FH3
51. R. Holzwarth, T. Udem, T.W. Hansch, J.C. Knight, W.J. Wadsworth, P.S.J. Russell, "Optical frequency synthesizer for precision spectroscopy", *Phys. Rev. Lett.* **85**, pp. 2264-2267, 2000
52. I. Hartl, X.D. Li, C. Chudoba, R.K. Ghanta, T.H. Ko, J.G. Fujimoto, J.K. Ranka, R.S. Windeler, "Ultrahigh-resolution optical coherence tomography using continuum generation in an air-silica microstructure fiber", *Opt. Lett.* **26**, pp. 608-610, 2001
53. H. Kano, H. Hamaguchi, "Characterization of a supercontinuum generated from a photonic crystal fiber and its application to coherent Raman spectroscopy", *Opt. Lett.* **28**, pp. 2360-2362, 2003
54. W.J. Wadsworth, J.C. Knight, A. Ortigosa-Blanch, J. Arriaga, E. Silvestre, P.S.J. Russell, "Soliton effects in photonic crystal fibres at 850nm", *Electron. Lett.* **36**, pp. 53-55, 2000
55. B.R. Washburn, S.E. Ralph, P.A. Lacourt, J.M. Dudley, W.T. Rhodes, R.S. Windeler, S. Coen, "Tunable near-infrared femtosecond soliton generation in photonic crystal fibres", *Electron. Lett.* **37**, pp. 1510-1512, 2001
56. J.H.V. Price, W. Belardi, T.M. Monro, A. Malinowski, A. Piper, D.J. Richardson, "Soliton transmission and supercontinuum generation in holey fiber, using a diode pumped ytterbium fiber source", *Opt. Express* **10**, pp. 382-387, 2002
57. D.T. Reid, I.C. Cormack, W.J. Wadsworth, J.C. Knight, P.S.J. Russell, "Soliton self-frequency shift effects in photonic crystal fibre", *J. Mod. Opt.* **49**, pp. 757-767, 2002
58. K.S. Abedin, F. Kubota, "Widely tunable femtosecond soliton pulse generation at a 10-GHz repetition rate by use of the soliton self-frequency shift in photonic crystal fiber", *Opt. Lett.* **28**, pp. 1760-1762, 2003
59. Z. Yusoff, J.H. Lee, W. Belardi, T.M. Monro, P.C. Teh, D.J. Richardson, "Raman effects in a highly nonlinear holey fiber: amplification and modulation", *Opt. Lett.* **27**, pp. 424-426, 2002
60. F. Vanholsbeeck, P. Emplit, S. Coen, "Complete experimental characterization of the influence of parametric four-wave mixing on stimulated Raman gain", *Opt. Lett.* **28**, pp. 1960-1962, 2003

61. J.H. Lee, Z. Yusoff, W. Belardi, M. Ibsen, T.M. Monro, D.J. Richardson, "Investigation of Brillouin effects in small-core holey optical fiber: lasing and scattering", *Opt. Lett.* **27**, pp. 927-929, 2002
62. H. Hundertmark, D. Kracht, D. Wandt, C. Fallnich, V.V.R.K. Kumar, A.K. George, J.C. Knight, P.S.J. Russell, "Supercontinuum generation with 200pJ laser pulses in an extruded SF6 fiber at 1560nm", *Opt. Express* **11**, pp. 3196-3201, 2003
63. T. Hasegawa, E. Sasaoka, M. Onishi, M. Nishimura, Y. Tsuji, M. Koshiba, "Hole-assisted lightguide fiber for large anomalous dispersion and low optical loss", *Opt. Express* **9**, pp. 681-686, 2001
64. B.J. Eggleton, C. Kerbage, P.S. Westbrook, R.S. Windeler, A. Hale, "Microstructured optical fiber devices", *Opt. Express* **9**, pp. 698-713, 2001
65. C. Kerbage, B.J. Eggleton," Tunable microfluidic optical fiber gratings", *Appl. Phys. Lett.* **82**, pp. 1338-1340, 2003
66. J.K. Sahu, C.C. Renaud, K. Furusawa, R. Selvas, J.A. Alvarez-Chavez, D.J. Richardson, J. Nilsson, "Jacketed air-clad cladding pumped ytterbium-doped fibre laser with wide tuning range", *Electron. Lett.* **37**, pp. 1116-1117, 2001
67. R. Selvas, J.K. Sahu, L.B. Fu, J.N. Jang, J. Nilsson, A.B. Grudinin, K.H. Yla-Jarkko, S.A. Alam, P.W. Turner, J. Moore, "High-power, low-noise, Yb-doped, cladding-pumped, three-level fiber sources at 980nm", *Opt. Lett.* **28**, pp. 1093-1095, 2003
68. W.J. Wadsworth, J.C. Knight, W.H. Reeves, P.S.J. Russell, J. Arriaga, "Yb^{3+}-doped photonic crystal fibre laser", *Electron. Lett.* **36**, pp. 1452-1454, 2000
69. K. Furusawa, T.M. Monro, P. Petropoulos, D.J. Richardson, "Modelocked laser based on ytterbium doped holey fibre", *Electron. Lett.* **37**, pp. 560-561, 2001
70. J.H.V. Price, K. Furusawa, T.M. Monro, L. Lefort, D.J. Richardson, "Tunable, femtosecond pulse source operating in the range 1.06-1.33μm based on an Yb^{3+}-doped holey fiber amplifier", *J. Opt. Soc. Amer. B* **19**, pp. 1286-1294, 2002
71. K. Furusawa, J.K. Sahu, T.M. Monro, D.J. Richardson, "A high efficiency, low threshold, erbium-doped holey optical fiber laser", *Proc. Conference on Lasers and Electro-Optics (CLEO'2003),* Baltimore, 2003, paper CTuP
72. J. Canning, N. Groothoff, E. Buckley, T. Ryan, K, Lyytikainen, J. Digweed, "All-fibre photonic crystal distributed Bragg reflector (PC-DBR) fibre laser", *Opt. Express* **11**, pp. 1995-2000, 2003
73. K. P. Hansen, "Dispersion flattened hybrid-core nonlinear photonic crystal fiber", *Opt. Express* **11**, pp. 1503-1509, 2003
74. T. P. Hansen, J. Broeng, S.E.B. Libori, E. Knudsen, A. Bjarklev, J.R. Jensen, H. Simonsen, "Highly birefringent index-guiding photonic crystal fibers", *IEEE Photon. Technol. Lett.* **13**, pp. 588-590, 2001
75. B.J. Mangan, J.C. Knight, T.A. Birks, P.S.J. Russell, A.H. Greenway, "Experimental study of dual-core photonic crystal fibre", *Electron. Lett.* **36**, pp. 1358-1359, 2000
76. W.N. MacPherson, J.D.C. Jones, B.J. Mangan, J.C. Knight, P.S.J. Russell, "Two-core photonic crystal fibre for Doppler difference velocimetry", *Opt. Commun.* **223**, pp. 375-380, 2003
77. A. Ortigosa-Blanch, J.C. Knight, W.J. Wadsworth, J. Arriaga, B.J. Mangan, T.A. Birks, P.S.J. Russell, "Highly birefringent photonic crystal fibers", *Opt. Lett.* **5**, pp. 1325-1327, 2000
78. K. Suzuki, H. Kubota, S. Kawanishi, M. Tanaka, M. Fujita, "Optical properties of a low-loss polarization-maintaining photonic crystal fiber", *Opt. Express* **9**, pp. 676-680, 2001
79. G. Millot, A. Suter, J.M. Dudley, L. Provino, R.S. Windeler, "Polarization mode dispersion and vectorial modulational instability in air-silica microstructure fiber", *Opt. Lett.* **27**, pp. 695-697, 2002
80. T. Ritari, T. Niemi, H. Ludvigsen, M. Wegmuller, N. Gisin, J.R. Folkenberg, A. Petterson, "Polarization-mode dispersion of large mode-area photonic crystal fibers", *Opt. Commun.* **226**, pp. 233-239, 2003
81. P.J. Bennett, T.M. Monro, D.J. Richardson, "Towards practical holey fiber technology: fabrication, splicing, modeling, and characterization", *Opt. Lett.* **24**, pp. 1203-1205, 1999
82. B. Bourliaguet, C. Pare, F. Emond, A. Croteau, A. Proulx, R. Vallee, "Microstructured fiber splicing", *Opt. Express* **11**, pp. 3412-3417, 2003
83. T. Kogure, K. Furusawa, J.H. Lee, T.M. Monro, D.J Richardson, "An erbium doped holey fiber amplifier and ring laser", *Proc. European Conference on Optical Communication (ECOC'2003),* Rimini, Italy, 2003, postdeadline paper Th4.1.1
84. N.A. Mortensen, J.R. Folkenberg, M.D. Nielsen, K.P. Hansen, "Modal cutoff and the V parameter in photonic crystal fibers", *Opt. Lett.* **28**, pp. 1879-1881, 2003
85. T. A. Birks, J.C. Knight, P.S.J. Russell, "Endlessly single-mode photonic crystal fiber", *Opt. Lett.* **22**, pp. 961-963, 1997
86. J. Broeng, D. Mogilevstev, S.E. Barkou, A. Bjarklev, "Photonic crystal fibers: a new class of optical waveguides", *Opt. Fiber Tech.* **5**, pp. 305-330, 1999
87. M.D. Nielsen, N.A. Mortensen, "Photonic crystal fiber design based on the V-parameter", *Opt. Express* **11**, pp. 2762-2768, 2003
88. M.D. Nielsen, N.A. Mortensen, J.R. Folkenberg, A. Bjarklev, "Mode field radius of photonic crystal fibers expressed by the V parameter", *Opt. Lett.* **28**, pp. 2309-2311, 2003
89. B.T. Kuhlmey, R.C. McPhedran, C.M. de Sterke, P.A. Robinson, G. Renversez, D. Maystre, "Microstructured optical fibers: where's the edge?", *Opt. Lett.* **27**, pp. 1684-1686, 2002
90. N. A. Mortensen, "Effective area of photonic crystal fibers", *Opt. Express* **10**, pp. 341-348, 2002
91. J.R. Folkenberg, N.A. Mortensen, K.P. Hansen, T.P. Hansen, H.R. Simonsen, C. Jakobsen, "Experimental investigation of cutoff phenomena in nonlinear photonic crystal fibers", *Opt. Lett.* **28**, pp. 1882-1884, 2003
92. G.P. Agrawal, *Nonlinear Fiber Optics*, 2nd edition, Academic Press, Inc., 1995
93. T.M. Monro, D.J. Richardson, N.G.R. Broderick, P.J. Bennett, "Modeling large air fraction holey optical fibers", *J. Lightwave Technol.* **18**, pp. 50-56, 2000

94. T. Sorensen, J. Broeng, A. Bjarklev, E. Knudsen, S.E. Barkou Libori, "Macro-bending loss properties of photonic crystal fibre", *Electron. Lett.* **37**, pp. 287-289, 2001
95. M.D. Nielsen, G. Vienne, J.R. Folkenberg, A. Bjarklev, "Investigation of microdeformation-induced attenuation spectra in a photonic crystal fiber", *Opt. Lett.* **28**, pp. 236-238, 2003
96. M. Ohashi, K. Shiraki, K. Tajima, "Optical loss property of silica-based single-mode fibers", *J. Lightwave Technol.* **10**, pp. 539-543, 1992
97. M. Ohashi, M. Tateda, K. Shiraki, K. Tajima, "Imperfection loss reduction in viscosity-matched optical fibers", *IEEE Photon. Technol. Lett.* **5**, pp. 812-814, 1993
98. K. Saitoh, M. Yamaguchi, H. Kakiuchida, A.J. Ikushima, K. Ohsono, Y. Kurosawa, "Limit of the Rayleigh scattering loss in silica fiber", *Appl. Phys. Lett.* **83**, pp. 5175-5177, 2003
99. K. Tajima, J. Zhou, K. Kurokawa, K. Nakajima, "Low water peak photonic crystal fibres", *Proc. European Conference on Optical Communication (ECOC'2003),* Rimini, Italy, 2003, postdeadline paper Th4.1.6
100. V. Finazzi, T.M. Monro, D.J. Richardson, "Small-core silica holey fibers: nonlinearity and confinement loss trade-offs", *J. Opt. Soc. Amer.* **B 20**, pp. 1427-1536, 2003
101. L. Farr, J.C. Knight, B.J. Mangan, P.J. Roberts, "Low loss photonic crystal fibre", *Proc. European Conference on Optical Communications (ECOC'02),* Copenhagen, Denmark, 2002, postdeadline paper PD1.3
102. K. Tajima, J. Zhou, N. Nakajima, K. Sato, "Ultra low loss and long length photonic crystal fiber", *Proc. Optical Fiber Communications Conference (OFC'2003),* Atlanta, Georgia, 2003, postdeadline paper PD1-1
103. J.C. Knight, J. Arriaga, T.A. Birks, A. Ortigosa-Blanch, W.J. Wadsworth, P.S.J. Russell, "Anomalous dispersion in photonic crystal fiber", *IEEE Photon. Technol. Lett.* **12**, pp. 807-809, 2000
104. J.H.V. Price, T.M. Monro, K. Furusawa, W. Belardi, J.C. Baggett, S. Coyle, C. Netti, J.J. Baumberg, R. Paschotta, D.J. Richardson, "UV generation in pure-silica holey fiber", *Appl. Phys. B* **77**, pp. 291-298, 2003
105. W.H. Reeves, D.V. Skryabin, F. Biancalana, J.C. Knight, P.S.J. Russell, F.G. Omenetto, A. Efimov, A.J. Taylor, "Transformation and control of ultra-short pulses in dispersion-engineered photonic crystal fibres", *Nature* **424**, pp. 511-515, 2003
106. J.D. Harvey, R. Leonhardt, S. Coen, G.K.L. Wong, J.C. Knight, W.J. Wadsworth, P.S.J. Russell, "Scalar modulation instability in the normal dispersion regime by use of a photonic crystal fiber", *Opt. Lett.* **28**, pp 2225-2227, 2003
107. A.V. Husakou, J. Herrman, "Supercontinuum generation of higher-order solitons by fission in photonic crystal fibers", *Phys. Rev. Lett.* **87**, 203901, pp. 1-4, 2003
108. A.V. Husakou, J. Herrmann, "Supercontinuum generation, four-wave-mixing, and fission of higher-order solitons in photonic-crystal fibers", *J. Opt. Soc. Amer. B* **19**, pp. 2171-2182, 2002
109. T. A. Birks, D. Mogilevstev, J.C. Knight, P.S.J. Russell, "Dispersion compensation using single-material fibers", *IEEE Photon. Tech. Lett.* **11**, pp. 674-676, 1999
110. L.-P. Shen, W.-P. Huang, G.X. Chen, S.S. Jian, "Design and optimization of photonic crystal fibers for broad-band dispersion compensation", *IEEE Photon. Technol. Lett.* **15**, pp. 540-542, 2003
111. A. Ferrando, E. Silvestre, J.J. Miret, P. Andres, "Nearly zero ultraflattened dispersion in photonic crystal fibers", *Opt. Lett.* **25**, pp. 790-792, 2000
112. A. Ferrando, E. Silvestre, P. Andres, J.J. Miret, M.V. Andres, "Designing the properties of dispersion-flattened photonic crystal fibers", *Opt. Express* **9**, pp. 687-698, 2001
113. W. H. Reeves, J.C. Knight, P.S.J. Russell, P.J. Roberts, "Demonstration of ultra-flattened dispersion in photonic crystal fibers", *Opt. Express* **10**, pp. 609-613, 2002
114. K. Saitoh, M. Koshiba, T. Hasegawa, E. Sasaoka, "Chromatic dispersion control in photonic crystal fibers: application to ultra-flattened dispersion", *Opt. Express* **11**, pp. 843-852, 2003
115. G. Renversez, B. Kuhlmey, R. McPhedran, "Dispersion management with microstructured optical fibers: ultraflattened chromatic dispersion with low losses", *Opt. Lett.* **28**, pp. 989-991, 2003
116. A. Peyrilloux, T. Chartier, A. Hideur, L. Berthelot, G. Melin, S. Lempereur, D. Pagnoux, P. Roy, "Theoretical and experimental study of the birefringence of a photonic crystal fiber", *J. Lightwave Technol.* **21**, pp. 536-539, 2003
117. H. Lim, F.O. Ilday, F.W. Wise, "Femtosecond ytterbium fiber laser with photonic crystal fiber for dispersion control", *Opt. Express* **10**, pp. 1497-1502, 2002
118. C.J.S. de Matos, S.V. Popov, J.R. Taylor, "Short-pulse, all-fiber, Raman laser with dispersion compensation in a holey fiber", *Opt. Lett.* **28**, pp. 1891-1893, 2003
119. A.V. Avdokhin, S.V. Popov, J.R. Taylor, "Totally fiber integrated, figure-of-eight, femtosecond source at 1605nm", *Opt. Express* **11**, pp. 265-269, 2003
120. T.M. Monro, D.J. Richardson, P.J. Bennett, "Developing holey fibres for evanescent field devices", *Electron. Lett.* **35**, pp. 1188-1189, 1999
121. Y.L Hoo, W. Jin, H.L. Ho, D.N. Wang, "Measurement of gas diffusion coefficient using photonic crystal fiber", *IEEE Photon. Technol. Lett.* **15**, pp. 1434-1436, 2003
122. M. Nakazawa, H. Kubota, K. Tamura, "Random evolution and coherence degradation of a high-order optical soliton train in the presence of noise", *Opt. Lett.* **24**, pp. 318-320, 1999
123. J. Hansryd, F. Dross, M. Westlund, P.A. Antrekson, S.N. Knudsen, "Increase of the SBS threshold in a short highly nonlinear fiber by applying a temperature distribution", *J. Lightwave Technol.* **19**, pp. 1048-1050, 2001